

1 **Extreme Events Across New Mexico During the 2018 North American**

2 **Monsoon**

3 Jorge Torres\*

4 *KOB-TV, Albuquerque, New Mexico*

5 Daniel Pagliaro

6 *Pagcore Solutions LLC, Albuquerque, New Mexico*

7 \*Corresponding author address: Jorge Torres, KOB-TV, 4 Broadcast Plaza SW, Albuquerque, NM

8 87104.

9 E-mail: jct\_02@msn.com

## ABSTRACT

10 The 2018 North American Monsoon season was characterized by localized  
11 severe storm and flash flood events in New Mexico. Notable events included  
12 flash flooding in Belen and parts of Rio Rancho on 5 July; inundation of San  
13 Antonio on 15 July; the 1,000-year flood event in and around Santa Fe on 23  
14 July; and a severe hail event in the Albuquerque area on 30 July. Analysis of  
15 these events was conducted to better understand the synoptic, mesoscale, and  
16 local conditions that contributed to their occurrence with the goal of helping  
17 forecasters better predict similar monsoon-driven severe storm and flash flood  
18 events in the future. Additionally, analysis of 464 reporting sites (to include 12  
19 ASOS/AWOS, 105 COOP, and 347 CoCoRaHS) across New Mexico revealed  
20 that most of the state experienced below average rainfall, with pockets of  
21 above average rainfall along and to the east of the central mountain chain  
22 during the 2018 North American Monsoon season. The rainfall distribution  
23 pattern developed as the prevalent monsoon pattern evolved from the Type II  
24 "reverse" monsoon pattern in July and early August to the "classic" Type I  
25 pattern in late August. The likely causes of the three flash flooding events in  
26 July 2018 stem from orographic uplift and outflow boundary interactions, and  
27 the diversion of arroyos and streams from their natural watercourses by human  
28 development. An amplified jet stream with embedded shortwave troughs that  
29 skirt across northern New Mexico is favored for severe thunderstorm activity  
30 across the state during the North American Monsoon season.

## 31 **1. Introduction**

32 Severe thunderstorms and flash flooding caused localized damage across New Mexico during  
33 the 2018 North American Monsoon season. Several flash flooding events resulted in extensive  
34 damage in the Middle Rio Grande Valley between 5 July 2018 and 30 July 2018, including the  
35 1,000-year flood event in the Santa Fe area on 23 July 2018; flash flooding and mudslides near Rio  
36 Rancho and Belen on 5 July 2018 and San Antonio on 16 July 2018; and a severe hail event that  
37 struck Albuquerque on 30 July 2018.

38 Previous studies of the North American Monsoon have largely focused on severe weather and  
39 flash flood impacts and attempts to improve forecasting monsoon events in Arizona and northwest-  
40 ern Mexico (Gochis et al. 2004; Gutzler et al. 2005; Maddox et al. 1995). Published research on  
41 the North American Monsoon's impacts in New Mexico is much more limited, with some research  
42 into local-scale monsoon behavior around the Los Alamos area (Bowen 1996), and synoptic-scale  
43 research encompassing the entirety of the American Southwest and northwestern Mexico (Adams  
44 and Comrie 1997). This paper attempts to associate rainfall patterns and major severe thunder-  
45 storm events across New Mexico to known synoptic-scale North American Monsoon regimes to  
46 help forecasters more accurately predict the characteristics of an upcoming monsoon season. Ad-  
47 ditionally, associating the synoptic-scale regime to major severe weather and flash flood events  
48 will help forecasters improve the day-to-day prediction of such events in New Mexico through  
49 pattern recognition.

## 50 **2. Background**

### 51 *a. New Mexico geography*

52 New Mexico's geography (Fig. 1) varies from the relatively flat plains in the east to the rugged  
53 mountains and plateaus in the central and western portions of the state. The lowest elevations are  
54 found along the lower Pecos River Valley in southeast New Mexico, while the highest elevations  
55 are located in the Sangre de Cristo Mountains of north-central New Mexico.

56 The western third of New Mexico is defined by the Colorado Plateau and the San Juan River  
57 Valley in the northwestern corner of the state, with mountainous terrain consisting of pine and  
58 juniper forests over the west-central, the basin-and-range province over the southwest corner and  
59 the New Mexico Bootheel. The Continental Divide runs north-to-south through the western part of  
60 New Mexico, from the Colorado border north of Chama, southwestward to near Gallup, and then  
61 through the Datil Mountains and Gila Wilderness to near Silver City, before reaching the Mexican  
62 Border southwest of Deming. Average elevations range from around 1,200 to 1,600 m in the San  
63 Juan Valley and southwest deserts to 2,100 m over the Northwest Plateau, to over 2,400 m in the  
64 Gila Wilderness, with mountain peaks as high as 3,600 m.

65 The central third of New Mexico is defined by the Rio Grande Valley, which runs north-to-  
66 south from the Colorado border north of Taos, to New Mexico's southern border south of Las  
67 Cruces. It has an average elevation ranging from 1,200 m in the south to over 1,800 m in the north.  
68 Immediately to the west of the Rio Grande Valley and approximately 75 km north of Albuquerque  
69 are the Jemez Mountains, which have an average elevation of 2,400 m with the highest peaks  
70 approaching 3,600 m. The Tusas Mountains begin north of the confluence of the Chama River  
71 and Rio Grande and run northward to west of the Rio Grande, extending into Colorado. To the  
72 east of the Rio Grande Valley is the central mountain chain, which consists of the Sangre de

73 Cristo Mountains in the north, the Sandia and Manzano Mountains in the central region, and the  
74 Sacramento Mountains to the south. The average height of these mountain ranges vary from 3,000  
75 m in the Sangre de Cristo range, to 2,300 m in the Sandia and Manzano range, to 2,600 m in  
76 the Sacramento Mountains, with the highest peaks ranging from 3,300 m to around 4,000 m in  
77 elevation.

78 The eastern portion of New Mexico is defined by the High Plains, and the eastern foothills of  
79 the central mountain chain. The Pecos River Valley runs northwest to southeast from west of Las  
80 Vegas, to Santa Rosa and Roswell, before crossing into Texas south of Carlsbad. Average elevation  
81 varies from 1,000 m to 1,200 m along the border with Texas to around 2,000 m at the eastern base  
82 of the central mountain chain near Raton, Las Vegas, Vaughn, and west of Roswell and Carlsbad.

### 83 *b. Characteristics of the North American Monsoon*

84 In New Mexico, the North American Monsoon season runs from 15 June to 30 September, and  
85 accounts for one-third to one-half of the state's annual precipitation (Douglas et al. 1993; NOAA  
86 n.d.).

87 Multiple papers (Adams and Comrie 1997; Bowen 1996; Douglas et al. 1993; Grantz et al. 2007)  
88 point out there are three sources of moisture for the North American Monsoon: the Gulf of Mexico,  
89 Pacific Ocean, and Gulf of California. Moisture from the Gulf of Mexico advects northwestward  
90 into eastern and central New Mexico due to southerly flow around the western periphery of the  
91 Bermuda High. With relatively flat terrain spanning the distance from the Texas Gulf Coast to  
92 New Mexico, moisture advection from the Gulf of Mexico encounters relatively little resistance  
93 making its way into New Mexico. In contrast, the moisture flow from the Pacific Ocean and  
94 Gulf of California is driven by the pressure gradient between the summertime thermal low that  
95 develops over the Mojave Desert and high pressure to the south. That pressure gradient creates

96 a low-level jet that advects tropical moisture northward from the Gulf of California and into the  
97 southwestern United States (Adams and Comrie 1997; Douglas et al. 1993). The Mogollon Rim of  
98 central Arizona and the Continental Divide that runs through far western New Mexico effectively  
99 preclude the bulk of the moisture originating from the Pacific Ocean and Gulf of California from  
100 penetrating deep into New Mexico (Bowen 1996). Thus, the greatest monsoon influence from the  
101 Pacific Ocean and Gulf of California is limited to portions of far western New Mexico that lie  
102 to the west of the Continental Divide, while the remainder of the state is mainly influenced by  
103 moisture from the Gulf of Mexico (Adams and Comrie 1997).

104 Previous studies, notably Maddox et al. (1995), have identified four major synoptic-scale pat-  
105 terns over the American Southwest during the North American Monsoon season. The following  
106 paragraphs tailor the monsoon pattern types as they apply to New Mexico.

#### 107 *Type I - Southern Plains/Four Corners High*

108 The Type I regime (Fig. 2) represents the "classic" monsoon pattern over New Mexico. Under  
109 the Type I regime, two high centers develop: one over the Southern Plains and a second centered  
110 around the Four Corners region (Maddox et al. 1995). Southerly flow between the two high cen-  
111 troids facilitates the northward advection of moisture through central New Mexico. Under this  
112 regime, convection typically favors the central mountain chain and Continental Divide. Storms  
113 will usually develop over the mountains and move in a northerly direction, with a slight compo-  
114 nent to the east or west, depending on the exact steering flow. This pattern is also favored for  
115 monsoon bursts with prolonged periods of widespread heavy rain that typically occur as easterly  
116 waves or the remnants of tropical systems from the Caribbean or Gulf of California are shunted  
117 northward across New Mexico between the two high centers.

118 *Type II - Great Basin High*

119 The Type II (Fig. 3) pattern is informally called the "reverse monsoon" pattern in New Mexico.  
120 This pattern features a strong high centroid in the vicinity of the Great Basin (although the high  
121 could be situated as far east as the Four Corners), with a deep trough positioned over the Great  
122 Plains and Mississippi Valley (Maddox et al. 1995). The prevailing steering flow with the Type  
123 II pattern over New Mexico is from the north, with a slight east or west component depending  
124 on the exact positioning of the synoptic-scale features. Under this regime, backdoor cold fronts  
125 commonly drop southward across the eastern plains of New Mexico, then push westward through  
126 the gaps in the central mountain chain before stalling near the Continental Divide. These cold  
127 fronts draw Gulf of Mexico moisture westward across the eastern plains, through the gaps of  
128 the central mountain chain and into the Rio Grande Valley. Strong easterly winds are usually  
129 associated with a frontal passage below the favored mountain gaps that open into the Rio Grande  
130 Valley. These easterly gap winds often will suppress major convective activity in the Albuquerque  
131 area due to the shadowing effect of downsloping despite the abundance of low-level moisture.  
132 Thunderstorms will typically initiate along the Continental Divide, Jemez and Tusas Mountains,  
133 and central mountain chain and propagate in a southerly direction toward the adjacent lowlands.

134 *Type III - Trapping High*

135 Under this regime (Fig. 4), a sprawling area of upper-level high pressure is centered directly  
136 over New Mexico and Arizona that suppresses moisture intrusions into New Mexico. This leads  
137 to mid-level warming temperatures, stronger subsidence, and forces the development of showers  
138 and storms to rely heavily on the recycling of low-level moisture already in place. Very light  
139 steering flow in this pattern leads to slow storm motions and increases the risk for flash flooding  
140 from highly localized, but intense rainfall (Maddox et al. 1995).

#### 141 *Type IV - Transitional*

142 The transitional pattern (Fig. 5) develops when the subtropical high over the Southern Plains  
143 is displaced to the south and east in response to an approaching shortwave trough and associated  
144 cold front from the west. Moisture flux and convection is consistent with typical pre-frontal pre-  
145 cipitation patterns observed elsewhere. A wind shift to the west or northwest and rapid cooling  
146 and drying occur following frontal passage (Maddox et al. 1995; NOAA n.d.).

### 147 **3. Methodology**

148 The objective of this study was to identify rainfall and severe thunderstorm distribution patterns,  
149 with respect to the prevailing synoptic-scale pattern. To accomplish this, an empirical analysis  
150 of meteorological data collected across New Mexico during the 2018 North American Monsoon  
151 season was analyzed. Particular focus was given to four major weather events that resulted in  
152 significant property damage. Additionally, available historical monsoon data covering the period  
153 from 1988 to 2017 was also analyzed in an attempt to associate the prevailing synoptic pattern to  
154 precipitation anomalies and severe thunderstorm activity identified in a particular year. The study  
155 covered the North American Monsoon season from 15 June to 30 September, a period of 108 days.

#### 156 *a. Data*

157 Data analyzed during this study included surface and upper-air analysis charts; National Cen-  
158 ters for Environmental Prediction (NCEP)/National Center for Atmospheric Research (NCAR)  
159 re-analysis data from 2000 to 2018 (Kalnay et al. 1996); rainfall data from National Weather Ser-  
160 vice (NWS) Automated Surface Observing System and Automated Weather Observing System  
161 (ASOS/AWOS) and Cooperative Observer Program (COOP) sites; rainfall data from the Commu-  
162 nity Collaborative Rain, Hail and Snow (CoCoRaHS) Network; satellite and NEXRAD radar im-



163 agery. Historical precipitation data for NWS surface observation and COOP sites, and NEXRAD  
164 radar imagery were obtained from the National Center for Environmental Information (NCEI).  
165 Long-term precipitation data was analyzed by using the Applied Climate Information System  
166 (ACIS) (Hubbard et al. 2004). Satellite imagery was accessed and analyzed using the NCEI's  
167 Global ISCCP B1 Browse System (GIBBS) (Knapp 2008). NEXRAD radar imagery from the  
168 three sites in New Mexico (Albuquerque, KABX; Cannon Air Force Base, KFDX; and Holloman  
169 Air Force Base, KHDX) and El Paso, Texas (KEPZ) were analyzed using the NCEI's Weather  
170 and Environmental Toolkit application. Upper-air soundings from Albuquerque (KABQ) for four  
171 major storm events on 5 July, 15-16 July, 23 July, and 30 July were analyzed using the Sounding  
172 and Hodograph Analysis and Research Program in Python (SHARPPy) (Blumberg et al. 2017).

173 Historical precipitation data for the CoCoRaHS network was obtained via the CoCoRaHS web-  
174 site. Precipitation reports were manually validated for each NWS ASOS/AWOS, COOP, and Co-  
175 CoRaHS site. Sites with less than 90 days of precipitation reports were excluded from further  
176 analysis. Sites with 90 to 107 days of precipitation reports were manually analyzed for days on  
177 which no reports were recorded versus precipitation reports that span multiple days. Precipitation  
178 amounts were estimated at sites on days when no report was submitted by either interpolation of  
179 precipitation amounts from nearby sites, or by NEXRAD Storm Total Precipitation estimates for  
180 sites in data-sparse locations. Precipitation and anomaly data were plotted using the Quantum  
181 Geographic Information System (QGIS) application.

182 The analysis of rainfall distribution for the 2018 monsoon season included data from 464 NWS  
183 ASOS/AWOS, COOP, and CoCoRaHS reporting sites across New Mexico. Of these, 12 were  
184 ASOS/AWOS stations, 105 were COOP locations, and 347 were CoCoRaHS sites.

185 Storm reports from the NWS Storm Prediction Center were also analyzed to characterize the  
186 distribution pattern for severe events, and associate severe storm distribution with respect to the

187 prevailing synoptic pattern using storm report and synoptic re-analysis information dating back to  
188 2000.

## 189 **4. Discussion**

### 190 *a. Evolution of the Synoptic-Scale Pattern*

191 In the early onset of the 2018 North American Monsoon, the 300 hPa high was situated near  
192 the Four Corners with periodic fluctuations across the Intermountain West. This ridge allowed  
193 surface cold fronts from the Great Plains to propagate westward into New Mexico, which resulted  
194 in moisture surges and increased wind shear. This set-up falls in line with the defined Type II or  
195 “Great Basin High” (Maddox et al. 1995; Kalnay et al. 1996).

196 The Type II pattern was dominant from early July through early August. In mid-August, the  
197 Great Basin High weakened and a new high centroid developed over Texas. As a result, the Type  
198 I pattern became prevalent for the latter half of August (Maddox et al. 1995; Kalnay et al. 1996).

199 Near the end of August, southwesterly flow strengthened over New Mexico in response to a  
200 deepening upper-level trough off the West Coast. The prevailing synoptic pattern transitioned to a  
201 Type IV setup by 31 August as the upper trough and associated Pacific cold front moved inland,  
202 shoving the high centroid over Texas eastward (Maddox et al. 1995; Kalnay et al. 1996).

### 203 *b. Distribution of Precipitation*

204 Precipitation amounts varied widely across New Mexico (Fig. 6) during the 2018 North Ameri-  
205 can Monsoon season. The lowest amounts (under 25 mm) were recorded on the Northwest Plateau  
206 in the vicinity of Farmington, while the highest rainfall amounts were reported around the south-  
207 ern end of the Sangre de Cristo Mountains near Las Vegas (over 400 mm), with locations in the  
208 Sacramento Mountains and Gila Wilderness recording 300 to 400 mm. Precipitation amounts in

209 the Rio Grande Valley and the southern deserts ranged from 50 to 200 mm, with sites in the eastern  
210 foothills of Albuquerque recording up to 300 mm of precipitation. Locations across the eastern  
211 plains varied from 100 to 250 mm, with most sites reporting around 200 mm of precipitation.

212 Precipitation anomalies for 93 NWS ASOS/AWOS and COOP sites across New Mexico were  
213 analyzed and plotted (Fig. 7). Departures from average varied from 30 percent of average on  
214 the northwest plateau at Farmington to 385 percent of average at the southern end of the Tusas  
215 mountain range near Canjilon. Of the 93 sites analyzed, 61 recorded below average precipitation,  
216 while above average rainfall was reported at 32 locations.

217 Most of New Mexico experienced below average precipitation, although there were scattered  
218 pockets of above average precipitation. The largest concentration of above average rainfall  
219 stretched from the eastern slopes of the Sangre de Cristo Mountains southeastward to the east-  
220 central plains, including the cities of Las Vegas, Santa Rosa, Fort Sumner, and Clovis. Other  
221 concentrations of above average precipitation were also recorded on the east side of the Albu-  
222 querre metro area, the Sandia and Manzano Mountains, and Sacramento Mountains. More iso-  
223 lated pockets of above average rainfall were reported in the Jemez and Tusas Mountains and in the  
224 northeastern corner of the state.

### 225 *c. Severe Storm Distribution*

226 Severe storm activity for the 2018 monsoon season was concentrated in the northeast quadrant of  
227 New Mexico (Fig. 8), although a smaller concentration of severe storm reports also occurred in the  
228 Albuquerque metro area. This is consistent with the storm behavior typically seen with the Type II  
229 pattern, as shortwave troughs moving southeastward from Colorado to the Texas Panhandle send  
230 backdoor cold fronts southward through northeastern New Mexico. The shortwave troughs help

231 draw moisture northwestward into New Mexico, while also providing sufficient vertical shear to  
232 initiate severe storm development along and behind the advancing cold fronts.

#### 233 *d. Major Events*

##### 234 *Rio Rancho and Belen Flash Floods, 5 July 2018*

235 Slow-moving thunderstorms developed over the Sandia and Manzano Mountains during the late  
236 afternoon of 5 July 2018. One cell formed over the north end of the Sandia range and drifted  
237 westward across the Rio Grande, resulting in up to 55 mm of rainfall in less than 90 minutes,  
238 and flash flooding in the northern part of Rio Rancho, particularly along U.S. Highway 550. A  
239 second cell formed over the Manzano Mountains around the same time as the first cell, and moved  
240 westward across the Rio Grande. Similar flash flooding occurred with up to 42 mm of rainfall  
241 reported in the town of Belen. Most of Belen was inundated with floodwaters due to a levee  
242 breach caused by the intense rainfall (NOAA 2018).

243 *(i) Synoptic Conditions* A modified Type I pattern was in place on 5 July 2018. A strong, but  
244 diffuse upper-level ridge was present over the Great Plains, with the high centroid located along  
245 the border between Nebraska and South Dakota. Meanwhile, a strong (600 dam at 500 hPa)  
246 high centroid was situated over the Four Corners region. The monsoon plume stretched from the  
247 Gulf of Mexico northwestward across central New Mexico in the weakness between the two high  
248 centroids, as evidenced on the 700 hPa dew point analysis at 05/1200 UTC and 06/0000 UTC (Fig.  
249 9a. and c.). The upper-level ridge axis was oriented across far northern New Mexico, resulting in  
250 light easterly flow over the Sandia and Manzano range and the adjacent middle Rio Grande Valley.  
251 Two shortwave troughs were propagating around the northern periphery of the subtropical ridge:  
252 one moving northeastward across western and northern Colorado, and a second that would move

253 from south-central Nebraska at 05/1200 UTC southwestward to southeast New Mexico by 06/0000  
254 UTC, as evidenced by GOES-15 water vapor imagery (Fig. 9b. and d.). Convection formed over  
255 the Sandia and Manzano Mountains by 05/2000 UTC in response to the approaching trough and  
256 orographic enhancement from easterly flow riding up the east-facing slopes of the range.

257 The steering flow would have directed any thunderstorms that formed over the Sandia and Man-  
258 zano range westward into the Rio Grande Valley. Orographic intensification occurred as the storms  
259 ascended the mesas to the west of the Rio Grande, enhancing rainfall amounts. This phenomenon  
260 did indeed occur in the case of the cell that impacted Rio Rancho. The collision of outflow bound-  
261 aries from these and other nearby cells helped spawn new cells that prolonged heavy rainfall  
262 around Rio Rancho and Belen.

#### 263 *San Antonio Flash Flood, 15 July 2018*

264 On the evening of 15 July 2018, heavy thunderstorm rainfall of up to 82 mm fell over the  
265 Chupadera Mountains of south-central New Mexico. This rainfall overwhelmed Walnut Creek,  
266 which is diverted into a series of irrigation ditches at the town of San Antonio, and resulted in  
267 a flash flood that inundated San Antonio with water and mud, washed out several roads, and  
268 damaged 20 homes and buildings (NOAA 2018).

269 *(ii) Synoptic Conditions* The predominant synoptic pattern over New Mexico on 15 July was  
270 the Type II regime, with an elongated high centroid stretching from the Great Basin westward  
271 into the eastern Pacific. A light northeasterly steering flow was present over New Mexico, with  
272 a large, but diffuse moisture plume covering the entire state at 700 hPa. The upper-air sounding  
273 from Albuquerque (KABQ) for 16/0000 UTC (Fig. 10) indicated marginally unstable conditions  
274 with a Most Unstable Convective Available Potential Energy (MUCAPE) value of  $574 \text{ j kg}^{-1}$ . A  
275 weak cap was present with a Most Unstable Convective Inhibition (MUCINH) value of  $24 \text{ j kg}^{-1}$ .

276 The Lifted Index was -1.88. Thunderstorm initiation over the lower Rio Grande Valley occurred  
277 with strong surface heating, with upslope enhancement over the Chupadera Mountains to the west.  
278 Although the 15 mm of rain that fell over San Antonio was significantly lower than the amount  
279 that fell over the Chupadera Mountains, flash flooding inundated San Antonio when heavy rain  
280 over the adjacent mountain range overwhelmed Walnut Creek.

281 *(iii) Diversion of Walnut Creek* Construction of a railroad, highways, and farms over the span  
282 of generations in an around San Antonio resulted in the lower portion of Walnut Creek being  
283 diverted from its original course that previously emptied into the Rio Grande, and into a series of  
284 ditches to irrigate adjacent farmland. At the railroad tracks, Walnut Creek's natural creek bed ends  
285 with a 90-degree southward turn into a ditch that begins immediately after passing underneath  
286 the railroad bridge. The ditch then runs along the north side of U.S. Highway 380 for a short  
287 distance before crossing under the highway and emptying into another irrigation ditch that runs  
288 parallel to the Rio Grande. Compared to the creek's original course, the ditches have much less  
289 capacity. More significantly, Walnut Creek no longer connects directly with the Rio Grande,  
290 rather it empties into a series of irrigation ditches that are separated from the river by a levee.  
291 This diversion exacerbated the inundation of San Antonio when Walnut Creek flooded, as the  
292 water from upstream was blocked from emptying into the Rio Grande, forcing the creek to flood  
293 adjacent farmland and the town of San Antonio.

#### 294 *Santa Fe Area Flash Floods, 23 July 2018*

295 During the early evening of 23 July 2018, several slow-moving thunderstorms developed across  
296 central and northern New Mexico. These storms produced torrential rainfall in the Santa Fe  
297 metropolitan area, resulting in devastating flash flooding. CoCoRaHS, COOP, and NWS observa-  
298 tion sites measured rainfall amounts between 16.5 mm of rain at the Santa Fe Municipal Airport

299 and 93.8 mm of rain in less than one hour near the Santa Fe Plaza, which equated to a 500-or  
300 1000-year precipitation event.

301 An upper-level ridge centered over the Desert Southwest on 23 July along with a weak surface  
302 backdoor cold front provided the necessary ingredients for record monsoonal rainfall in and near  
303 the New Mexico capitol. This unprecedented heavy rain event resulted in 10 roads closed and  
304 100 homes damaged due to flooding. Of those 100 homes, 33 experienced major damage with six  
305 destroyed (NOAA 2018).

306 *(iv) Synoptic Conditions* A modified Type I pattern was present over New Mexico, with the upper  
307 high centroid at 300 hPa straddling the border between southeast New Mexico and West Texas.  
308 With the westward displacement of the high centroid, relatively dry air infiltrated much of central  
309 and southern New Mexico at the mid-and upper-levels. The richest moisture associated with the  
310 monsoon plume was shunted into central Arizona, then curving northeastward into northwest and  
311 north-central New Mexico. With the high centroid nearby, the steering flow at 500 hPa over New  
312 Mexico was light, generally from a westerly direction over northern and central parts of the state,  
313 and from an easterly direction over extreme southern New Mexico.

314 A backdoor cold front stalled along the Continental Divide, and was undergoing frontolysis.  
315 Temperatures were particularly hot across north-central New Mexico, with the Santa Fe Municipal  
316 Airport reporting a temperature of 32.7 °C by 24/0000 UTC. From the Albuquerque sounding at  
317 23/1200 UTC (Fig. 11), the atmosphere was marginally unstable with a MUCAPE value of 216 J  
318 kg<sup>-1</sup> and a MUCINH value of 418 J kg<sup>-1</sup>. The convective temperature was 27.2 °C, which was  
319 easily exceeded by mid-afternoon. By 24/0000 UTC (Fig. 12) the MUCAPE had increased to  
320 1082 J kg<sup>-1</sup> and the MUCINH had decreased to 5 J kg<sup>-1</sup>. Meanwhile, abundant moisture was

321 present as evidenced by the precipitable water value of 22.1 mm at 23/1200 UTC, which increased  
322 to 23.1 mm by 24/0000 UTC.

323 Thunderstorm initiation was largely driven by surface heating, as most of New Mexico was  
324 under the influence of the upper-level high centered over the southern part of the state. By mid-  
325 afternoon, thunderstorms developed over the Jemez Mountains and along the Continental Divide  
326 when the surface temperature exceeded the convective temperature to initiate thunderstorm devel-  
327 opment. A low-level southerly flow fed moisture into the developing storms, while a light westerly  
328 steering flow at and above 500 hPa directed the cells southeastward toward the upper Rio Grande  
329 Valley and the Santa Fe area. New cells formed along outflow boundaries that spread out from  
330 older thunderstorms. The particular cell that caused the flash flood over Santa Fe formed as a re-  
331 sult of an outflow boundary colliding with the low-level southerly inflow. Orographic uplift along  
332 the southern end of the Sangre de Cristo Mountains helped enhance the intensity of the Santa Fe  
333 storm, resulting in 93.8 mm of rain and flash flooding near the Santa Fe Plaza. The village of La  
334 Cienega, about 25 km southwest of the Santa Fe Plaza, received substantially less rainfall, but the  
335 village was inundated with floodwaters when Cienega Creek became a raging torrent due to the  
336 intense rainfall kilometers upstream.

337 *Albuquerque Severe Hail, 30 July 2018*

338 Two severe thunderstorms dropped hail up to 32 mm in diameter across the east side of Albu-  
339 querque during the evening of 30 July 2018. The first cell developed over the Northeast Heights  
340 and moved south-southeastward toward the Four Hills area. The second cell formed over the city  
341 of Rio Rancho, then intensified as it moved south over the North Valley neighborhoods before  
342 reaching downtown Albuquerque. This cell weakened as it continued southward over the Albu-  
343 querque International Sunport and Kirtland Air Force Base. Hail from the two cells damaged cars



344 throughout the Albuquerque metro area. One person was treated for injuries caused by the hail  
345 (NOAA 2018).

346 *(v) Synoptic Conditions* On 30 July 2018, a Type II monsoon pattern was present with the high  
347 centroid situated over the Great Basin, and a broad upper-level trough situated over the Upper  
348 Midwest (Maddox et al. 1995). At 30/1200 UTC, a  $45 \text{ m s}^{-1}$  jet streak at 300 hPa was located  
349 over north-central Colorado (Fig. 13a). This jet streak supported a shortwave trough moving  
350 southeastward through northern Colorado. A strong backdoor cold front pushed westward through  
351 the gaps in the central mountain chain, resulting in strong easterly gap winds of up to  $17 \text{ m s}^{-1}$   
352 at the Albuquerque International Sunport (KABQ). The front reached the Continental Divide later  
353 in the morning. A very dry air mass was in place over the Four Corners region. As Gulf moisture  
354 surged westward behind the front, the vertical profile of the front itself became more characteristic  
355 of a dry line. Surface dew points over the Four Corners were below  $0 \text{ }^\circ\text{C}$ , while dew points to  
356 the east of the Continental Divide approached  $16 \text{ }^\circ\text{C}$  in the Rio Grande Valley, with higher values  
357 reported to the east of the central mountain chain.

358 Isolated convection developed during the afternoon of 30 July over the highlands of west-central  
359 New Mexico, the Jemez Mountains, and Tusas and Sangre de Cristo Mountains of northern New  
360 Mexico. The steering flow at 500 hPa was from northwest to southeast. The flow at 300 hPa  
361 was more westerly, while the low-level flow from the surface to 700 hPa was generally from the  
362 southeast. By the evening of 30 July (31/0000 UTC), the core of the 300 hPa jet streak—now  $38$   
363  $\text{m s}^{-1}$ —was situated near Amarillo, Texas (Fig. 13b). The associated shortwave trough at 500 hPa  
364 stretched from the Texas Panhandle westward to east-central New Mexico. The backdoor front  
365 stalled along the Continental Divide and completely transformed to a dry line as depicted by the  
366 sharp moisture gradient.

367 The synoptic setup over New Mexico was favorable for the initiation of severe convection. The  
368 backdoor front advected ample Gulf of Mexico moisture into eastern and central New Mexico. The  
369 same front also forced the Great Basin High to retreat westward, reducing upper-level subsidence  
370 and increasing instability as reflected by the surface-based CAPE value of  $1,399 \text{ J kg}^{-1}$  and CINH  
371 of  $97 \text{ J kg}^{-1}$  from the 31/0000 UTC upper-air sounding at Albuquerque (Fig. 14). The trajectory of  
372 the jet streak at 300 hPa would have skirted through the northeast corner of New Mexico, placing  
373 the Albuquerque metro area close to the right-entrance region of this feature, where upper-level  
374 divergence would be present. The jet streak and mid-level trough interacting with the surface  
375 dry line provided sufficient lift and vertical shear to initiate convection over the Jemez Mountains  
376 to the north-northwest of the Albuquerque metro area. The steering flow directed these cells  
377 southeastward over the Albuquerque metro area. A moist, southeasterly flow below 700 hPa,  
378 combined with west-northwesterly flow at 300 hPa provided sufficient vertical shear to enable  
379 rapid intensification and sustainment of strength as the cells moved from the Jemez Mountains  
380 into the Rio Grande Valley.

## 381 **5. Conclusion**

382 The 2018 North American Monsoon season started with a Type II pattern that evolved to a  
383 Type I regime from mid-August onward. Consistent with the Type II regime, the majority of New  
384 Mexico experienced below average precipitation, although there were scattered pockets of above  
385 average rainfall that favored the eastern slopes of the central mountain chain and the east side of  
386 the Albuquerque metro area. While there were no widespread severe storm or flash flood events in  
387 2018, several localized flash flood and a severe hail storm caused injuries and property damage to  
388 locations in the Rio Grande Valley.

389 Storm activity that produced flash flooding was enhanced by orographic uplift and perpetuated  
390 by colliding outflow boundaries. In two of the three flash flood events, the heaviest rainfall oc-  
391 curred kilometers upstream of the locations subject to the most destructive flooding. Diversion of  
392 a waterway from its natural watercourse by human development was a major factor in at least one  
393 of the flash flood events in this study.

394 Finally, the Albuquerque severe hail event of 30 July 2018 was attributable to a synoptic pattern  
395 where a backdoor cold front swept westward across New Mexico, stalled near the Continental  
396 Divide, and evolved into a dry line. This study concludes that where a backdoor cold front stalls  
397 becomes a focal point for severe storms under the Type II regime. This is particularly the case  
398 when the jet stream is in close proximity to New Mexico and embedded shortwave troughs skirt  
399 through the state and interact with the frontal boundary. In response, upper-level divergence and  
400 vertical shear enhance storm initiation, intensification, and longevity.

## 401 **6. Acknowledgements**

402 The authors would like to thank Mr. Kerry Jones from the National Weather Service Forecast  
403 Office in Albuquerque, and Dr. David DuBois from the New Mexico State Climatologist's Office  
404 in Las Cruces for taking the time to peer review this manuscript and validate the findings contained  
405 herein.

## 406 **References**

- 407 Adams, D. K., and A. C. Comrie, 1997: The North American Monsoon. *Bulletin of the American*  
408 *Meteorological Society*, **78 (10)**, 2197–2214.
- 409 Blumberg, W. G., K. T. Halbert, T. A. Supinie, P. T. Marsh, R. L. Thompson, and J. A. Hart, 2017:  
410 SHARPPy: An open-source sounding analysis toolkit for the atmospheric sciences. *Bulletin of*

411 *the American Meteorological Society*, **98 (8)**, 1625–1636.

412 Bowen, B. M., 1996: Rainfall and climate variation over a sloping New Mexico plateau during the  
413 North American Monsoon. *Journal of Climate*, **9 (12)**, 3432–3442.

414 Douglas, M. W., R. A. Maddox, K. Howard, and S. Reyes, 1993: The Mexican Monsoon. *Journal*  
415 *of Climate*, **6 (8)**, 1665–1677.

416 Gochis, D. J., A. Jimenez, C. J. Watts, J. Garatuza-Payan, and W. J. Shuttleworth, 2004: Analysis  
417 of 2002 and 2003 warm-season precipitation from the North American Monsoon Experiment  
418 event rain gauge network. *Monthly Weather Review*, **132 (12)**, 2938–2953.

419 Grantz, K., B. Rajagopalan, M. Clark, and E. Zagona, 2007: Seasonal shifts in the North American  
420 Monsoon. *Journal of Climate*, **20 (9)**, 1923–1935.

421 Gutzler, D. S., and Coauthors, 2005: The North American Monsoon Model Assessment Project:  
422 Integrating numerical modeling into a field-based process study. *Bulletin of the American Me-*  
423 *teorological Society*, **86 (10)**, 1423–1430.

424 Hubbard, K. G., A. T. DeGaetano, and K. D. Robbins, 2004: A modern applied climate informa-  
425 tion system. *Bulletin of the American Meteorological Society*, **85 (6)**, 811.

426 Kalnay, E., and Coauthors, 1996: The NCEP/NCAR reanalysis 40-year project. *Bull. Am. Meteo-*  
427 *rol. Soc.*, **77 (3)**, 437–471.

428 Knapp, K. R., 2008: Scientific data stewardship of International Satellite Cloud Climatol-  
429 ogy Project B1 global geostationary observations. *Journal of Applied Remote Sensing*, **2 (1)**,  
430 023 548.

431 Maddox, R. A., D. M. McCollum, and K. W. Howard, 1995: Large-scale patterns associated with  
432 severe summertime thunderstorms over central Arizona. *Weather and Forecasting*, **10** (4), 763–  
433 778.

434 NOAA, 2018: The Top 5 Weather Stories of 2018 (NWS Albuquerque, NM).  
435 <https://www.weather.gov/abq/TheTop5WeatherStoriesof2018> (Accessed April 8, 2019).

436 NOAA, n.d.: North American Monsoon patterns for New Mexico.  
437 <https://www.weather.gov/abq/northamericanmonsoon-typicalpatterns> (Accessed October  
438 12, 2018).

439 **LIST OF FIGURES**

440 **Fig. 1.** Map of New Mexico with major geographic features annotated. . . . . 23

441 **Fig. 2.** Synoptic depiction for the Type I "classic" monsoon pattern. The typical location of the  
442 monsoon moisture plume is depicted in green. The green arrow indicates the direction of  
443 moisture flux. Adapted from Maddox et al. (1995) and NOAA (n.d.). . . . . 24

444 **Fig. 3.** Synoptic depiction for the Type II "reverse" monsoon pattern. The typical location of the  
445 monsoon moisture plume is depicted in green. The green arrow indicates the direction of  
446 moisture flux. Adapted from Maddox et al. (1995) and NOAA (n.d.). . . . . 25

447 **Fig. 4.** Synoptic depiction for the Type III monsoon pattern. The typical location of the monsoon  
448 moisture plume is depicted in green. Adapted from Maddox et al. (1995) and NOAA (n.d.). . . . 26

449 **Fig. 5.** Synoptic depiction for the Type IV monsoon pattern. The typical location of the monsoon  
450 moisture plume is depicted in green. The green arrow indicates the direction of moisture  
451 flux. Adapted from Maddox et al. (1995) and NOAA (n.d.). . . . . 27

452 **Fig. 6.** Precipitation distribution across New Mexico from the 2018 North American Monsoon sea-  
453 son. . . . . 28

454 **Fig. 7.** Precipitation anomalies across New Mexico from the 2018 North American Monsoon sea-  
455 son. . . . . 29

456 **Fig. 8.** SPC severe storm reports for New Mexico during the 2018 North American Monsoon sea-  
457 son. . . . . 30

458 **Fig. 9.** 700 hPa analysis and water vapor imagery for 1200 UTC 5 July 2018 (a. and c., respec-  
459 tively), and 0000 UTC 6 July 2018 (b. and d. respectively) (Knapp 2008). . . . . 31

460 **Fig. 10.** Albuquerque (KABQ) upper-air sounding for 0000 UTC 16 July 2018. . . . . 32

461 **Fig. 11.** Albuquerque (KABQ) upper-air sounding for 1200 UTC 23 July 2018. . . . . 33

462 **Fig. 12.** Albuquerque (KABQ) upper-air sounding for 0000 UTC 24 July 2018. . . . . 34

463 **Fig. 13.** 300 hPa analysis for 1200 UTC 30 July 2018 (a) and 0000 UTC 31 July 2018 (b). . . . . 35

464 **Fig. 14.** Albuquerque (KABQ) upper-air sounding for 0000 UTC 31 July 2018. . . . . 36

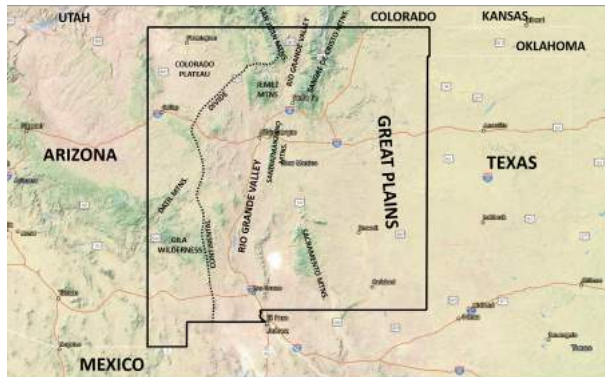
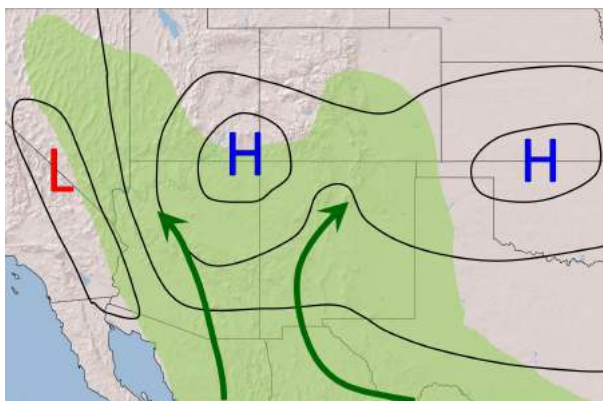
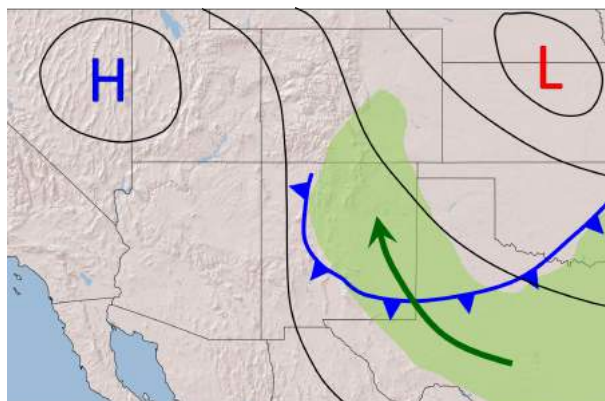


FIG. 1. Map of New Mexico with major geographic features annotated.

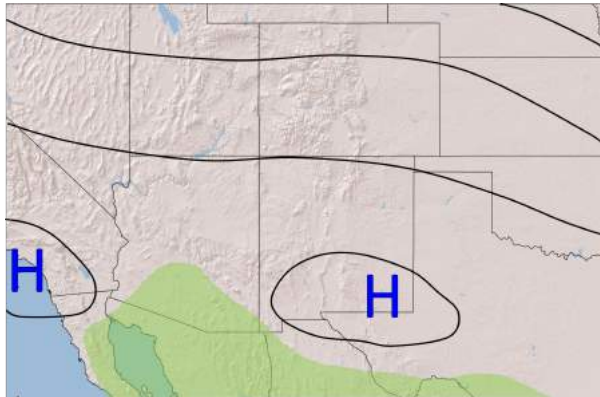


465 FIG. 2. Synoptic depiction for the Type I "classic" monsoon pattern. The typical location of the monsoon  
466 moisture plume is depicted in green. The green arrow indicates the direction of moisture flux. Adapted from  
467 Maddox et al. (1995) and NOAA (n.d.).

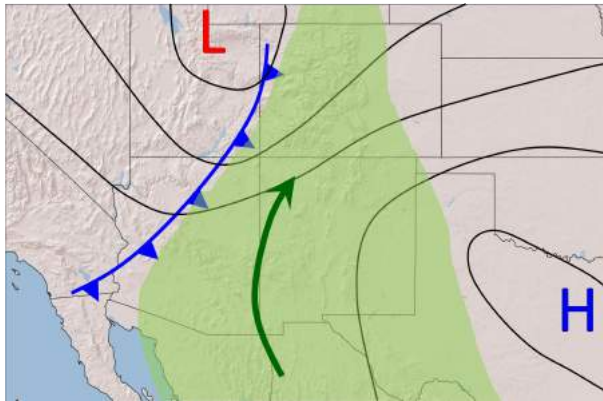




468 FIG. 3. Synoptic depiction for the Type II "reverse" monsoon pattern. The typical location of the monsoon  
469 moisture plume is depicted in green. The green arrow indicates the direction of moisture flux. Adapted from  
470 Maddox et al. (1995) and NOAA (n.d.).



471 FIG. 4. Synoptic depiction for the Type III monsoon pattern. The typical location of the monsoon moisture  
472 plume is depicted in green. Adapted from Maddox et al. (1995) and NOAA (n.d.).



473 FIG. 5. Synoptic depiction for the Type IV monsoon pattern. The typical location of the monsoon moisture  
474 plume is depicted in green. The green arrow indicates the direction of moisture flux. Adapted from Maddox  
475 et al. (1995) and NOAA (n.d.).

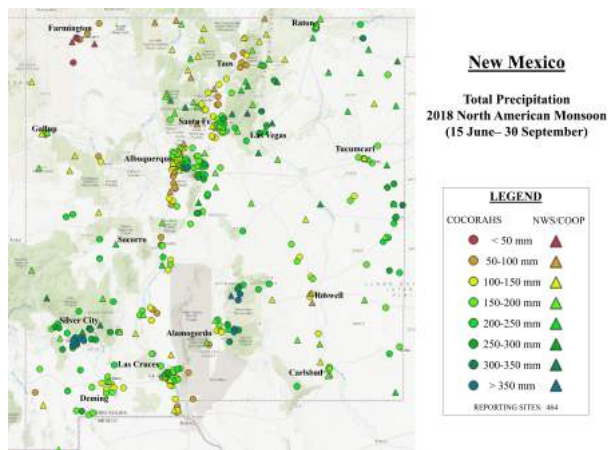


FIG. 6. Precipitation distribution across New Mexico from the 2018 North American Monsoon season.

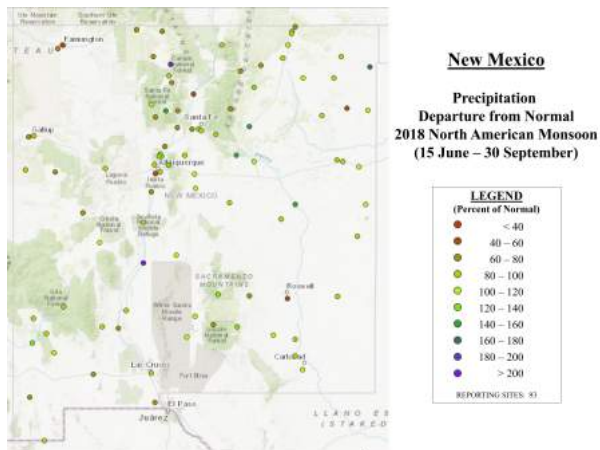


FIG. 7. Precipitation anomalies across New Mexico from the 2018 North American Monsoon season.

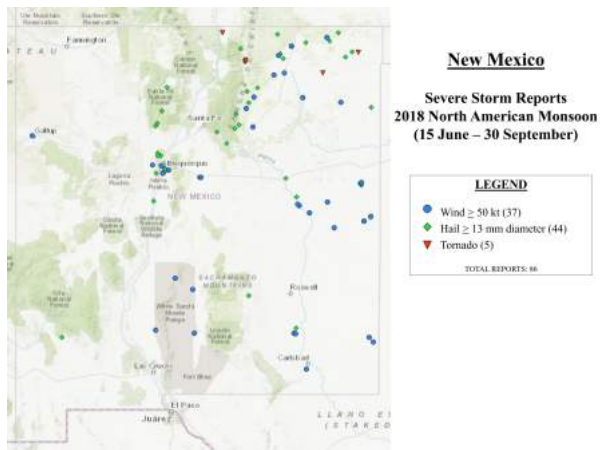
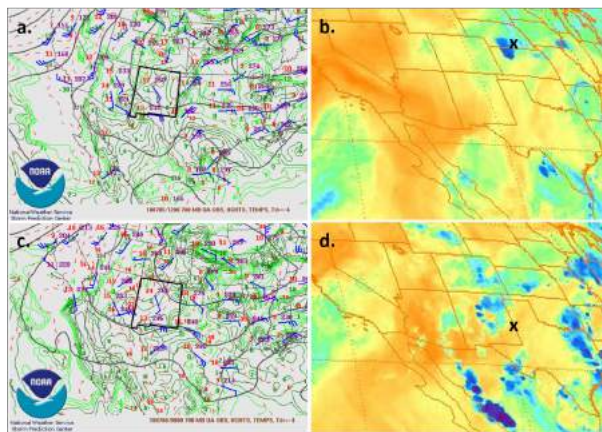


FIG. 8. SPC severe storm reports for New Mexico during the 2018 North American Monsoon season.



476 FIG. 9. 700 hPa analysis and water vapor imagery for 1200 UTC 5 July 2018 (a. and c., respectively), and  
 477 0000 UTC 6 July 2018 (b. and d. respectively) (Knapp 2008).

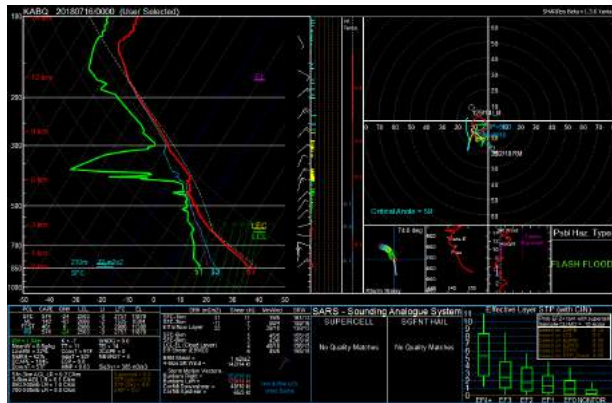


FIG. 10. Albuquerque (KABQ) upper-air sounding for 0000 UTC 16 July 2018.



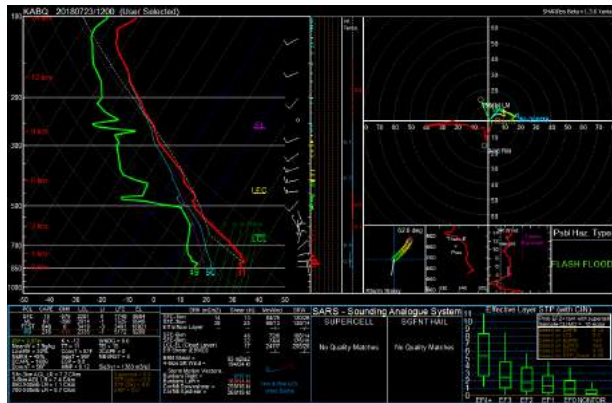


FIG. 11. Albuquerque (KABQ) upper-air sounding for 1200 UTC 23 July 2018.

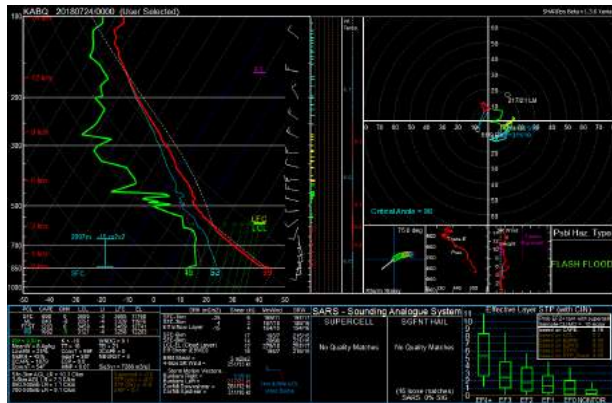


FIG. 12. Albuquerque (KABQ) upper-air sounding for 0000 UTC 24 July 2018.

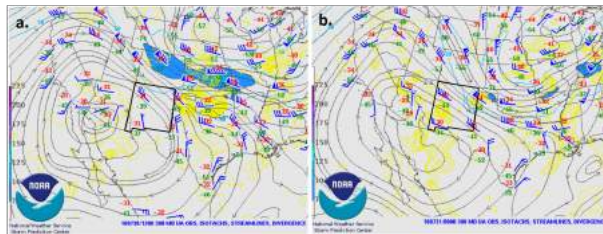


FIG. 13. 300 hPa analysis for 1200 UTC 30 July 2018 (a) and 0000 UTC 31 July 2018 (b).

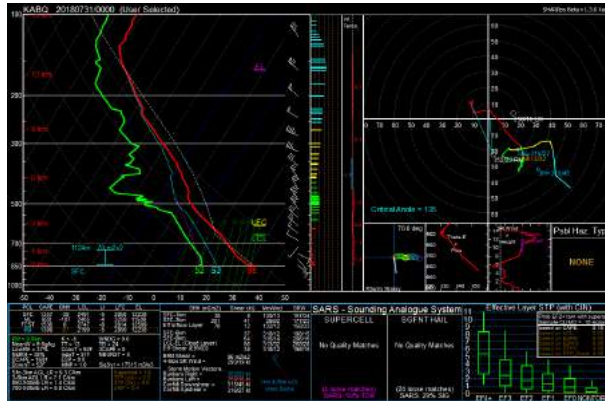


FIG. 14. Albuquerque (KABQ) upper-air sounding for 0000 UTC 31 July 2018.